Progress In Electromagnetics Research, PIER 40, 155–176, 2003

MODE TRANSFIGURATIONS IN CHIROWAVEGUIDES

G. I. Komar' and A. Y. Poyedinchuk

Usikov Institute for Radiophysics & Electronics
National Academy of Sciences of Ukraine (IRE NASU)
12 Academic Proskura Street, 61085, Kharkov, Ukraine

Abstract—it has been analyzed physical features of the modes behavior in a waveguide filled with the chiral medium. Both mathematical and physical models of their propagation have been defined and modes classification has been suggested. It has been shown that the same root feature in dispersion is typical both for chirowaveguide modes and for the unchiral waveguide; however the mode transfiguration is peculiar to all chirowaveguide modes and this determines the complex character of the final dispersion curves behavior. The following features are typical for chirowaveguide modes: connections between polarizations and between wave types, intersections of the dispersion curves, the spatial beatings and consecutive changes of the eigen function while moving the operating point along the dispersion curve (the mode transfiguration). The chirowaveguide performs polarization selection of propagating waves in such a way that only right-polarized waves can exist under big values of propagation constant in the chirowaveguide; the mode transfiguration is the reason of this.

1. INTRODUCTION

The properties of the chiral and biisotropic media [1–3] and electromagnetic structures based on these media are still under discussion in literature [4–6]. In the works [7–12] it has been solved the problems concerning waves in a parallel plate chirowaveguide (see Fig. 1a) [7–9], in a circular metal chirowaveguide [5, 10], in a circular dielectric chirowaveguide [5, 10] and in a microstrip line on the chiral substrate [11]. The problem of wave propagation in the circular biisotropic waveguide has been solved in [5]. The problem of the rectangular chirowaveguide excitation has been considered in [12].

In particular it has been shown that only hybrid waves can propagate in chirowaveguides and transverse electric (TE) waves, transverse magnetic (TM) waves or transverse electromagnetic (TEM) waves cannot be supported in a chirowaveguide [7–10]. The dispersion curves for chirowaveguides have been obtained and it has been shown that these curves behave in an unusual way, not as in a usual waveguide [7–9]. The phenomenon of dispersion curves splitting called mode bifurcation has been described [7–9]. The frequency dispersion of the transverse wave numbers has been observed [7, 8]. The mode with zero cutoff frequency has been discovered in a parallel-plate chirowaveguide and it has been analyzed in the work [9]. More detailed bibliography concerning this question can be found in [5, 6].

In the works [7–12] the problem statement and peculiarities of its solving in case when a waveguide is filled with the chiral medium are stated in detail. However these works do not give consideration to the physical processes taking place in such electrodynamic structures. At the same time the chirowaveguide physics has a whole series of principal features. The chirowaveguide waves are not identical to the waves in usual waveguides. Our problem is to obtain asymptotic correlations from the rigorous solution, in the mathematical sense, and from the heuristic approach, and we must compare them. It will allow us to differentiate physical processes that lead to the atypical behavior of the chirowaveguides dispersion curves. We shall consider a chirowaveguide not so much from the mathematical point of view as from the radiophysical one. We shall endeavor the physical and mathematical models to supplement each other.

2. THE FIELD REPRESENTATION IN AN INFINITE CHIRAL MEDIUM

The chiral medium is a variety of the artificial dielectric and consists of the ideal non-dispersive isotropic unchiral dielectric — the medium-matrix with parameter $\varepsilon\mu$, in which three-dimensional chiral figures have been molded [3, 5], and $\varepsilon = \varepsilon_c\varepsilon_0$, $\mu = \mu_c\mu_0$ are the absolute permittivity and permeability of the medium-matrix. The parameter γ is referred to as a chirality admittance. Material equations, which describe the isotropic chiral medium, can be written as in [3]:

$$\vec{D} = \varepsilon_c\varepsilon_0\vec{E} - i\gamma\sqrt{\varepsilon_0\mu_0}\vec{H}, \quad \vec{B} = \mu_c\mu_0\vec{H} + i\gamma\sqrt{\varepsilon_0\mu_0}\vec{E}. \tag{1}$$

The time t dependence has been chosen as $e^{-i\omega t}$. One can see the alternative methods of material equations introduction in [5].

So if the linearly polarized wave $E_x = A'\cos(\omega t - k_c z)$ propagating in a dielectric with parameter $\varepsilon\mu$ gets into the chiral medium based on the same dielectric, it will split into two waves with circular polarization: the left-hand circularly polarized (LHCP) plane wave E_{-x}, E_{-y} and the right-hand circularly polarized (RHCP) plane wave E_{+x}, E_{+y} (see Fig. 1b), and we add the sign (+) to RHCP and the sign (−) — to LHCP. Using the conventional form of the circular polarization wave representation [13] we write:

$$\begin{cases} E_{-x} = A'\cos(\omega t - k\_z), \\ E_{-y} = B'\sin(\omega t - k\_z) \end{cases} \qquad \begin{cases} E_{+x} = C'\cos(\omega t - k_+ z), \\ E_{+y} = -D'\sin(\omega t - k_+ z) \end{cases} \tag{2}$$

where $\omega = 2\pi c/\lambda_0$ is the circular frequency of the electromagnetic field; λ_0 is the free-space wavelength; $c = 1/\sqrt{\varepsilon_0\mu_0}$ is the velocity of light in vacuum;

$$k_\pm = \omega\left[\sqrt{\varepsilon\mu} \pm \gamma\sqrt{\varepsilon_0\mu_0}\right] = k_c(1 \pm \eta); \tag{3}$$

is the dispersion of the plane electromagnetic waves in the infinite homogeneous lossless isotropic chiral medium, $k_c = \omega\sqrt{\varepsilon\mu} = k_0\sqrt{\varepsilon_c\mu_c} = 2\pi/\lambda_c$ is the wavenumber for the isotropic unchiral medium with parameter $\varepsilon_c\mu_c k_0 = 2\pi/\lambda_0$ is the free-space wavenumber, λ_c is the wavelength in the isotropic unchiral medium with parameter $\varepsilon_c\mu_c$ (where wavevectors $\vec{k}_0, \vec{k}_c$ are directed along the $0Z$-axis), and $\eta = \gamma/\sqrt{\varepsilon\mu}$ is the relative parameter of chirality.

This splitting is conditioned by changing of the wave propagation speed: LHCP wave begins to pass ahead of the linearly polarized wave (the phase speed $V_{-f} = c/(\sqrt{\mu_c\varepsilon_c} - \gamma\ ) > V_f = c/\sqrt{\mu_c\varepsilon_c}$); and RHCP wave begins to remain behind the linearly polarized wave ($V_{+f} = c/(\sqrt{\mu_c\varepsilon_c} + \gamma\ ) < V_f$). However it is possible to obtain another

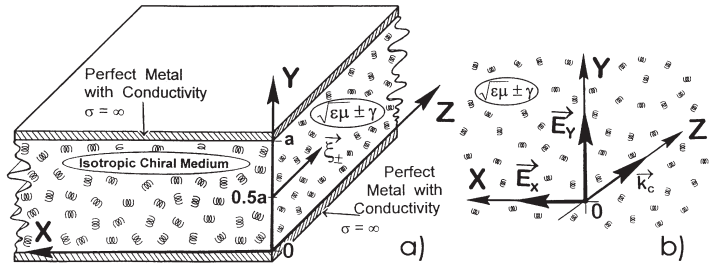

Figure 1. The electrodynamic structures considered in the paper: a) parallel-plate chirowaveguide; b) infinite chiral medium and chosen coordinate frame.

representation of waves in the infinite chiral medium. We sum up the circularly polarized waves (2). Then we obtain the system of two linearly polarized waves:

$$\begin{cases} E'_x = 2\cos(k_c\eta z)\cos(\omega t - k_c z) \\ E'_y = 2\sin(k_c\eta z)\cos(\omega t - k_c z). \end{cases} \tag{4}$$

The wave, polarization of which is changing continuously, corresponds to the system (4). When $z = p\pi/k_c\eta$ (where $p = 0, 1, 2, \ldots$) the wave will be linearly polarized ($E'_y = 0$); when $z = [1/2 + p]\pi/k_c\eta$ the wave will be linearly polarized too (but now $E'_x = 0$); when $z = [1/4+p]\pi/k_c\eta$ the wave will be the LHCP one; when $z = [3/4+p]\pi/k_c\eta$ the wave will be the RHCP one; in other cases it will be polarized elliptically. The system (4) can be interpreted in other terms too. The record (4) is typical for two coupled modes (for example, in the coupled transmission lines [14, 15]) and for spatial beatings of these two waves (the power is transferred in turn from E'_y to E'_x and vice versa):

$$\begin{cases} E'_x = \cos(K_S z)\cos(\omega t - k_c z) \\ E'_y = \sin(K_S z)\cos(\omega t - k_c z), \end{cases} \tag{5}$$

where the coefficient $K_S = k_c\eta$ that is equal to the product of the wavenumber and relative parameter of chirality is a coupling coefficient of polarizations E'_y and E'_x of one wave. Evidently the wave (5) has the wave vector $\vec{k}_c$ and propagates at the speed V_f, but the spatial beatings take place: the wave power is transferred in turn from one polarization to another at the length $L_S = \pi/2K_S = \pi/2k_c\eta$ that is also determined by the value η. It is significant that $K_S = \Delta k/2 = (k_+ - k_-)/2$ as in

[14, 15]. Then we obtain:

$$k_{\pm} = k_c \pm K_S. \tag{6}$$

The records (2) and (5) are identical for the case of the infinite chiral medium, but in case of a chirowaveguide they lead to two different types of dispersion. Let us consider this case in detail.

3. THE MODES OF THE PARALLEL-PLATE CHIRIWAVEGUIDE — THE RIGOROUS ANALYSIS

The parallel-plate chirowaveguide under investigation is formed by two layers of the perfect metal with conductivity $\sigma = \infty$ and by the layer of the homogeneous lossless isotropic non-dispersive chiral medium with thickness a, which is situated between them (see Fig. 1a and [8, 9]). Let us consider the rigorous, in the mathematical case, statement of the spectral problem of modes of the parallel-plate chirowaveguide with perfect electric walls. We shall obtain analytic solutions of this problem for two extreme situations when $\omega \to 0$ and $\omega \to \infty$ what can help us to analyze the physical features of the chirowaveguide dispersion in comparison with the results of heuristic buildings.

Let us assume that the fields of chirowaveguide modes are independent of the coordinate x (see Fig. 1a). Then on the basis of the Maxwell equations and material equations (1) it is possible to formulate the spectral problem where one should determine values of the spectral parameter $\xi_{[\pm n]}$ of the propagation constant, that allow the existence of non-trivial solutions of the following equations [7, 8]

$$\frac{d^2U_+}{dy^2} + \left(k_+^2 - \xi_{[\pm n]}^2\right) U_+ = 0, \quad \frac{d^2U_-}{dy^2} + \left(k_-^2 - \xi_{[\pm n]}^2\right) U_- = 0, \tag{7}$$

and that satisfy the boundary conditions on the chirowaveguide walls

$$(U_+ + U_-)|_{y=0,a} = 0, \quad \left[\frac{1}{1+\eta}\frac{dU_+}{dy} - \frac{1}{1-\eta}\frac{dU_-}{dy}\right]\Bigg|_{y=0,a} = 0. \tag{8}$$

From the Maxwell equations and from the relations (1) it follows that components of the E and H fields of modes can be expressed using the functions $U_{\pm}(y)$ by the following formulas:

$$\begin{aligned} E_x &= (U_+ + U_-)\exp(i\xi_{[\pm n]}z), \\ H_x &= -(i/W)(U_+ - U_-)\exp(i\xi_{[\pm n]}z), \\ E_y &= \frac{i\xi_{[\pm n]}}{k_c}\left(\frac{U_+}{1+\eta} - \frac{U_-}{1-\eta}\right)\exp(i\xi_{[\pm n]}z), \end{aligned}$$

$$
\begin{aligned}
H_y &= \frac{\xi_{[\pm n]}}{W k_c}\left(\frac{U_+}{1+\eta}+\frac{U_-}{1-\eta}\right)\exp(i\xi_{[\pm n]}z),\\
E_z &= \frac{1}{k_c}\left(\frac{1}{1-\eta}\frac{dU_-}{dv}-\frac{1}{1+\eta}\frac{dU_+}{dv}\right)\exp(i\xi_{[\pm n]}z),\\
H_z &= \frac{i}{W k_c}\left(\frac{1}{1+\eta}\frac{dU_+}{dy}+\frac{1}{1-\eta}\frac{dU_-}{dy}\right)\exp(i\xi_{[\pm n]}z),
\end{aligned}
\tag{9}
$$

where $W=\sqrt{(\mu_c\mu_0)/(\varepsilon_c\varepsilon_0)}$. The dispersion equations for $\xi_{[\pm n]}$ are obtained from (7) and (8) and look as follows:

$$y_-\cos y_+\sin y_- + [(1-\eta)/(1+\eta)]\,y_+\sin y_+\cos y_- = 0, \tag{10}$$

$$y_-\sin y_+\cos y_- + [(1-\eta)/(1+\eta)]\,y_+\cos y_+\sin y_- = 0, \tag{11}$$

where

$$y_\pm^2=\left(k_\pm^2-\xi_{[\pm n]}^2\right)a^2/4. \tag{12}$$

The values $y_\pm$ are non-dimensional transverse wavenumbers that describe the mode dependence on the coordinate y. It is necessary to add to the dispersion equations (10) and (11) the equation

$$y_+^2-y_-^2=(k_c a)^2\eta. \tag{13}$$

which follows from (12). Thus having determined transverse wavenumbers $y_\pm$ from (10), (13) or from (11), (13) one can calculate the propagation constants $\xi_{[\pm n]}^2=k_\pm^2-4y_\pm^2/a^2$. In [8] three regions of changing of the spectral parameter $\xi_{[\pm n]}$ were determined for the chirowaveguide propagating modes ($\xi_{[\pm n]}$ is the real number): $A=\{\xi_{[\pm n]}:\xi_{[\pm n]}\le k_-\}$; $B=\{\xi_{[\pm n]}:k_-\le\xi_{[\pm n]}<k_+\}$; $C=\{\xi_{[\pm n]}:\xi_{[\pm n]}>k_+\}$. It is easy to show that there are no solutions of the dispersion Equations (10)–(13) in the region C that correspond to the propagating modes. Actually, as $\xi_{[\pm n]}>k_+$, then $y_\pm=i\alpha_\pm$, where $\alpha_\pm$ are the real numbers. Substituting these values of $y_\pm$ for example, in (10), we shall obtain:

$$(1+\eta)\alpha_-\tanh\alpha_- + (1-\eta)\alpha_+\tanh\alpha_+ = 0. \tag{14}$$

As $0\le\eta\le 1$, then the left side of (14) is strongly positive for all $\alpha_\pm\neq 0$ and it follows from (13) that $\alpha_\pm\neq 0$, quod erat demonstrandum.

Let us transform the equations (10)–(13) for each of the regions A and B into the form convenient for the analytical and numerical analysis. Let $\xi_{[\pm n]}^2\in A$, then the transverse wavenumbers $y_\pm$ are the real ones. It is easy to see that if the pair (y_+,y_-) is the solution of

the equations (10), (13) (or (11), (13)), then the pair $(\pm y_+, \pm y_-)$ has this property too. So it is sufficient to consider the case when $y_\pm \geq 0$. In this case it follows from (13) that:

$$y_+ = k_c a\tau, \quad y_- = k_c a\sqrt{\tau^2 - \eta}, \tag{15}$$

where the parameter $\tau \geq \sqrt{\eta}$. Substituting the equation (15) into (10) and (11) we obtain two dispersion equations respectively:

$$\begin{aligned}
&\sqrt{\tau^2 - \eta}\cos k_c a\tau \sin\left(k_c a\sqrt{\tau^2 - \eta}\right) \\
&+(1-\eta)/(1+\eta)\tau \sin k_c a\tau \cos\left(k_c a\sqrt{\tau^2 - \eta}\right) = 0, \qquad (16) \\
&\sqrt{\tau^2 - \eta}\sin k_c a\tau \cos\left(k_c a\sqrt{\tau^2 - \eta}\right) \\
&+(1-\eta)/(1+\eta)\tau \cos k_c a\tau \sin\left(k_c a\sqrt{\tau^2 - \eta}\right) = 0. \qquad (17)
\end{aligned}$$

Let $\tau_0 \geq \sqrt{\eta}$ be the solution of the equation (16) or (17), then

$$\xi_{[\pm n]} a = k_c a\sqrt{(1+\eta)^2 - 4\tau_0^2}, \tag{18}$$

is the solution of the spectral problem (7) and (8). As far as $\xi_{[\pm n]}$ is the real number the variation domain of the parameter τ should coincide with the interval $[\sqrt{\eta}, (1+\eta)/2]$. It is easy to see that the value $\tau_0 = (1+\eta)/2$ is the root of the equation (16) (or (17)) only when $k_c a = \pi n, n = 0, 1, 2, \ldots$. In fact, substituting τ_0 into (16) and (17) we obtain: $\sin k_c a(\tau_0 + \sqrt{\tau_0^2 - \eta}) = 0$ and, consequently $k_c a = \pi n$. The values of the parameter $k_c a = \pi n$ are critical values, under which the propagation constants vanish.

Let $\xi_{[\pm n]} \in B$ now. Then the wavenumber y_- will be the imagine one and y_+ will be the real one. From (13) we obtain:

$$y_+ = \rho\cos\varphi, \quad y_- = i\rho\sin\varphi \tag{19}$$

where $\rho = k_c a\sqrt{\eta} = K_S a/\sqrt{\eta}$. As in the case of the A region it is enough to suppose that $y_+ \geq 0$, $Im\, y_- \geq 0$ and, consequently, the parameter φ will vary in the interval $[0, \pi/2]$. Taking into account the equation (19), the equations (10), (11) are transformed to the form:

$$\sin\varphi\cos(\rho\cos\varphi)\tanh(\rho\sin\varphi) - (1-\eta)/(1+\eta)\cos\varphi\sin(\rho\cos\varphi) = 0, \tag{20}$$

$$\sin\varphi\sin(\rho\cos\varphi)+(1-\eta)/(1+\eta)\cos\varphi\cos(\rho\cos\varphi)\tanh(\rho\sin\varphi)=0. \tag{21}$$

If $\varphi_0\in[0,\pi/2]$ is the root of the equation (20) (or (21)), then

$$\xi_{[\pm n]}a=k_ca\sqrt{(1+\eta)^2-4\eta\cos^2\varphi_0}, \tag{22}$$

is the solution of the problem (7), (8).

Let us investigate solutions of the equation (20) when $\rho\to 0$. For that let us represent (20) in the form of

$$1-\cos^2\varphi\frac{2}{1+\eta}+\rho^2\left(1+\sin^2\varphi-\frac{2\eta\cos^4\varphi}{1+\eta}\right)+0(\rho^2)=0,$$

where $0(\rho^2)/\rho^2\to 0$ when $\rho\to 0$. Using the Newton method it is easy to obtain the solution of this equation when $\rho\to 0$

$$\cos\varphi_0=\sqrt{(1+\eta)/2}\left[1-\rho^2[(1-\eta)(3+\eta)/2]+0(\rho^2)\right]. \tag{23}$$

Substituting (23) into (22) we shall obtain the following formula for the propagation constant

$$\xi_{[0]}=k_c\sqrt{1-\eta^2}\left[1-\eta(3+\eta)^2\rho^2+0\left(\rho^2\right)\right]. \tag{24}$$

From (24) it follows that the critical frequency of this mode is equal to zero (see [9] too). The structure of the electromagnetic field of this wave has the following form when $\rho\to 0$:

$$\begin{aligned}
E_x &= -A_1\left[\rho^2y/a(1-y/a)+0(\rho^2)\right]\exp\left(i\xi_{[0]}z\right),\quad E_z=0\left(\rho^2\right),\\
E_y &= iA_1\left[\left(1-\eta^2\right)^{-1/2}+\left(\rho^2/4\right)\sqrt{(1-\eta)(1+\eta)}+0\left(\rho^2\right)\right]\exp\left(i\xi_{[0]}z\right),\\
H_x &= -\left(iA_1/W\right)\left[1+\rho^2(0.25\,(1-\eta)+\eta(1-y/a)y/a)\,0\left(\rho^2\right)\right]\\
&\quad\exp\left(i\xi_{[0]}z\right),\\
H_y &= -\frac{A_1}{W}\left[\eta\left(1-\eta^2\right)^{-1/2}+\rho^2\left(0.25\eta\sqrt{(1-\eta)(1+\eta)}\right.\right.\\
&\quad\left.\left.-\sqrt{1-\eta^2}(1-y/a)y/a\right)+0\left(\rho^2\right)\right]\exp\left(i\xi_{[0]}z\right),\\
H_z &= \left(iA_1/W\right)\left(\rho(1-2y/a)+0\left(\rho^2\right)\right)\exp\left(i\xi_{[0]}z\right).
\end{aligned} \tag{25}$$

Here A_1 is the constant. Passing on (25) to the limit $\eta\to 0$ we obtain the electromagnetic field of the TEM-mode of the parallel-plate

unchiral waveguide [16]

$$\begin{aligned} E_y &= iA_1 \exp\left(i\xi_{[0]}z\right), \qquad H_x = -\left(iA_1/W\right)\exp\left(i\xi_{[0]}z\right), \\ E_x &= E_z = H_y = H_z = 0, \qquad \xi_{[0]} = k_c. \end{aligned} \tag{26}$$

We should stress that the $\xi_{[0]}$-wave is linearly polarized under the little a, since the quasistatic wave cannot have the circular polarization when $a < \lambda_0/2$.

4. THE MODES OF THE PARALLEL-PLATE CHIROWAVEGUIDE — THE HEURISTIC APPROACH

Let us apply the approach considered in Section 1 for the case of the chiral medium, which is confined by the planes of the parallel-plate chirowaveguide. We'll define the Brillouin's waves for our chirowaveguide in the usual way [16]. In Fig. 2 the forming of the Brillouin's waves in the parallel-plate chirowaveguide is shown for two cases: Fig. 2a — for the case of slightly coupled modes of two circular polarizations; Fig. 2b — for the case of strongly coupled modes of circular polarizations. Under large $\xi_{[\pm n]}$ (in B-region) in the case of slightly coupled E_x and E_y polarizations we shall use the following representation for the wavenumbers of the plane wave: $k_\pm = k_c(1 \pm \eta)$ (see (3)). It follows from Fig. 2a that the longitudinal wavenumber of the Brillouin's wave is $\xi_\pm = k_\pm \sin\theta_\pm$ where $\theta_\pm$ are angles of incidence of the plane Brillouin's waves (2) with wave vectors $k_\pm$ respectively. As $\cos\theta_\pm = \lambda_\pm/2a$ (where $\lambda_\pm = 2\pi/k_\pm$) we obtain $\xi_\pm = k_\pm\sqrt{1-\cos\theta_\pm} = \sqrt{k_c^2(1\pm\eta)^2 - (\pi/a)^2}$ or in the general case

$$\xi_{\pm m} = \sqrt{k_c^2\left(1\pm\eta\right)^2 - (m\pi/a)^2}; \quad \text{where } m = 1, 2, 3, \ldots \tag{27}$$

we obtain the Brillouin's waves dispersion in the parallel-plate chirowaveguide in case of slight coupling. At the same time the relative parameter of chirality is included in the effective dielectric permittivity $\varepsilon_{eff} = \varepsilon_c(1\pm\eta)^2$. Then $\xi_{\pm m} = \sqrt{k_0^2\varepsilon_{eff} - (m\pi/a)^2}$. The dispersion curves look like two branches that get out from different points $k_c a = m\pi/(1\pm\eta)$ or $k_0 a = m\pi/\varepsilon_{eff}$.

Under little $\xi_{[\pm n]}$ (in A-region) in case of strongly coupled E_x and E_y polarizations we shall use another representation for the wavenumbers of plane waves: $k_\pm = k_c \pm K_S$ (see (6)). It is convenient to denote the wavenumber for the case of strongly coupled Brillouin's waves with the letter ζ, which is different from ξ, but looks like it. It follows from Fig. 2b that the longitudinal wavenumber of the

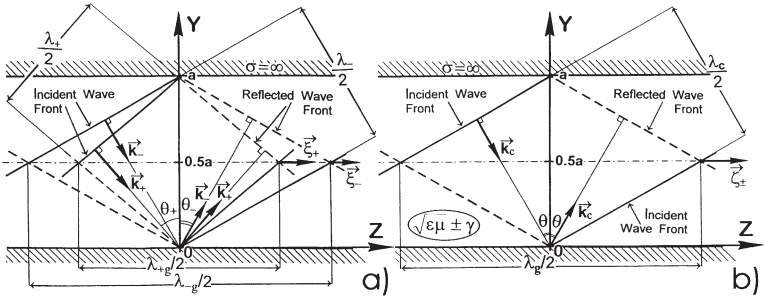

Figure 2. The Brillouin's waves in the parallel-plate chirowaveguide: a) for the case of slightly coupled $\xi_{\pm}$–waves; b) for the case of strongly coupled $\zeta_{\pm}$–waves; (where $\lambda_{\pm g} = 2\pi/\xi_{\pm}$ and $\lambda_g = 2\pi/\zeta$ are wavelengths in the waveguide for different types of dispersion; $\lambda_c = 2\pi/k_c$ is a wavelength in the non-chiral medium-matrix and $\lambda_{\pm} = 2\pi/k_{\pm}$ are lengths of the RHCP and LHCP waves in the infinite chiral medium).

Brillouin's wave (for this case) is $\zeta_{\pm} = k_{\pm}\sin\theta$, where θ is the angle of incidence of the sum of plane Brillouin's waves (5) and the wave vector k_c. Since $\cos\theta = \lambda_c/2a$ we shall obtain $\zeta_{\pm} = k_{\pm}\sqrt{1-\cos\theta} = \sqrt{k_c^2 - (\pi/a)^2}(1 \pm \eta)$ or in the general case

$$\zeta_{\pm n} = \sqrt{k_c^2 - (n\pi/a)^2}(1 \pm \eta);\ \text{where } n = 1, 2, 3, \ldots \qquad (28)$$

we shall obtain the Brillouin's waves dispersion in the parallel-plate chirowaveguide in case of strong coupling. At the same time the relative parameter of chirality η plays the role of the coupling coefficient K_n between the waves ζ_{+n} and ζ_{-n}: $K_n = \eta\sqrt{k_c^2 - (n\pi/a)^2}$; the dispersion of the coupling coefficient from $K_n = 0$ under $k_c a = n\pi$ to $K_n \to k_c\eta$ under $k_c a \to \infty$ can be seen; the dispersion curves look like two branches that get out from one point $k_c a = n\pi$. If we take into account that $h_n = \sqrt{k_c^2 - (n\pi/a)^2}$ is the dispersion in the unchiral parallel-plate waveguide [17] then $K_n = h_n\eta$ and $\zeta_{\pm n} = h_n \pm K_n$. The coupling coefficient is equal again to the product of the wavenumber and relative parameter of chirality. And if in the coupled transmission lines the coupling coefficient is determined by the gap dimension between the lines [14] and can be expressed using some coupling capacity [15], then in our case it is determined by parameters of the hiral medium and by the wavenumber in the unchiral medium-matrix. The magnitude L_S will be different for each n: $L_S = \pi/2K_n = \pi/2h_n\eta$. Under little $\xi_{[\pm n]} \to 0$ the operating wavelength is determined by the value h_n, not

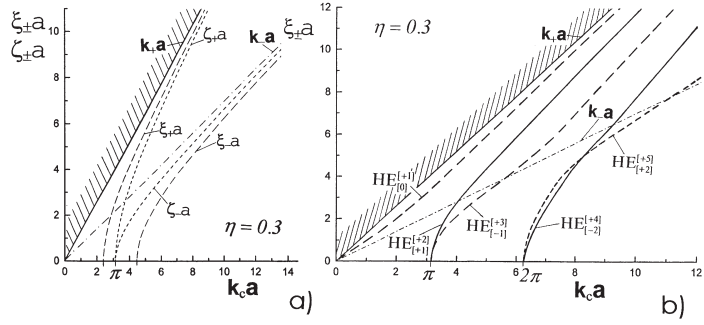

Figure 3. The dispersion in the parallel-plate chirowaveguide: a) ξ-dispersion (27) and ζ-dispersion (28) for $\eta = 0.3$; *b*) the dispersion of the first five modes of the chirowaveguide by the results of the strong analysis from (10) — the dot curves and from (11) — the solid curves.

by $\zeta_{\pm n}$ or $\xi_{\pm n}$. And therefore (and also due to $K_n \to 0$ under $\xi_{[\pm n]} \to 0$ critical wavelengths in the chirowaveguide are equal exactly to critical wavelengths in the unchiral (usual) waveguide.

In Fig. 3a all four dispersion curves $\zeta_{\pm n}$ and $\xi_{\pm n}$ for $n = 1$ are shown. It can be seen that $\zeta_{\pm n}$ get out from the point $k_c a = \pi$ and $\xi_{\pm n}$ get out from points $k_c a = \pi/(1 + \eta)$ and $k_c a = \pi/(1 - \eta)$ respectively. At that the curves, which correspond to the indice sign $(-)$ tend asymptotically to the line $k_c a = k_- a$ and the curves, which correspond to the sign $(+)$, tend to the line $k_c a = k_+ a$. It is clear that in the parallel-plate unchiral waveguide the waves h_n are converted to plane linearly polarized waves when $k_c a \to \infty$; so in the same case the $\zeta_{\pm n}$, $\xi_{\pm n}$-waves are asymptotically converted to waves of the infinite unchiral medium: to the LHCP and RHCP plane waves with dispersion (3). For further analyzing it is important that we can observe the situation under any n: four curves $\zeta_{\pm n}$, $\xi_{\pm n}$ will group around points with appropriate $n\pi$, at that ζ_{-n}, ξ_{-n} will deviate to the left, tending asymptotically to k_{-a}, and ζ_{+n}, ξ_{+n} will go steeply upwards crossing the curves ζ_{-n}, ξ_{-n} of the smaller index and tending asymptotically to k_{+a}. Then we obtain that any waves cannot propagate in the chirowaveguide under $\xi_{[\pm n]} > k_+$ (in the region C); when $k_- < \xi_{[\pm n]} < k_+$ (in the region B) only RHCP waves can propagate; when $\xi_{[\pm n]} < k_-$ (in A-region) both RHCP and LHCP waves can propagate.

5. RESULTS CONSIDERATION

Now let us compare the results obtained in Sections 2, 3 and 4 and analyze the physical reasons of the unusual behavior of the chirowaveguide dispersion curves. Let us consider Fig. 3b, which shows the final dispersion curves of five lowest modes of the parallel-plate chirowaveguide obtained from the mathematically rigorous dispersion equations (16) and (17). At that solid curves in Fig. 3b were obtained from (16) and the dashed ones were obtained from (17). It can be seen that the dispersion curves are splintered to pairs and have typical inflections and intersections. The dispersion curves of unchiral waveguides behave usually simpler. The phenomenon of dispersion curves splitting to pairs has been referred to as a mode bifurcation in the works [7–10]. In this work in Section 3 it is shown that the splitting is connected with the coupling effect between E_x and E_y polarizations (see (28)) of the chirowaveguide wave. From the results of the rigorous solution one can obtain the asymptotic result, which does not contradict this assertion. And so let us investigate the mode dispersion near critical points $k_c a = n\pi$. Let n be the integer positive number. Then for the small values of $|k_c a - n\pi| \ll 1$, using the Newton method one can obtain the following analytic solution of the equations (16) and (17)

$$\tau_{\pm n} = ((1+\eta)/2)\left[1 - \gamma_{\pm n}(k_c a - \pi n) + 0(k_c a - \pi n)\right], \qquad (29)$$

where $0(k_c a - n\pi)/(k_c a - n\pi) \to 0$ under $(k_c a - n\pi) \to 0$, and $\gamma_{\pm n} = (1-\eta^2)[(1-\eta^2)\pi n \pm 2\eta(-1)^n \sin(\pi n \eta)]^{-1}$, $n = 1, 2, \ldots$, when the sign $(+)$ corresponds to the roots of the equation (16) and the sign $(-)$ corresponds to the roots of the equation (17). Substituting the equation (29) into (18) we shall obtain

$$\xi_{[\pm n]} a = k_c a(1+\eta)\sqrt{2\gamma_{\pm n}(k_c a - \pi n)}\left(1 + 0\left(|k_c a - \pi n|^{1/2}\right)\right), \quad (30)$$

From (29) and (30) it follows that at the small neighborhood of values $k_c a = n\pi$ the existing propagation constants $\xi_{[\pm n]}$ vanish when $k_c a = n\pi$. Accurate within $0(|k_c a - n\pi|^{1/2})$ the structure of electromagnetic fields of these modes looks like:

$$\begin{aligned}
E_{+x} &= A_2 \sin(\pi n y/a) \sin(\pi n \eta y/a) \exp\left(i\xi_{[+n]} z\right), \\
E_{-x} &= iB_2 \sin(\pi n y/a) \cos(\pi n \eta y/a) \exp\left(i\xi_{[-n]} z\right), \\
E_{+y} &= H_{+y} = 0(|k_c a - n\pi|^{1/2}) \approx 0, \\
E_{-y} &= H_{-y} = 0(|k_c a - n\pi|^{1/2}) \approx 0,
\end{aligned}$$

$$
\begin{aligned}
E_{+z} &= -A_2 \sin(\pi n y/a) \cos(\pi n \eta y/a) \exp\left(i\xi_{[+n]} z\right), \\
E_{-x} &= iB_2 \sin(\pi n y/a) \sin(\pi n \eta y/a) \exp\left(i\xi_{[-n]} z\right), \\
H_{+x} &= (iA_2/W) \cos(\pi n y/a) \cos(\pi n \eta y/a) \exp\left(i\xi_{[+n]} z\right), \\
H_{-x} &= (B_2/W) \cos(\pi n y/a) \sin(\pi n \eta y/a) \exp\left(i\xi_{[-n]} z\right), \\
H_{+z} &= (iA_2/W) \cos(\pi n y/a) \sin(\pi n \eta y/a) \exp\left(i\xi_{[+n]} z\right), \\
H_{-z} &= -(B_2/W) \cos(\pi n y/a) \cos(\pi n \eta y/a) \exp\left(i\xi_{[-n]} z\right), \quad (31)
\end{aligned}
$$

where A_2, B_2 are constants. It is essential for our analysis that the dispersion equation (30), which corresponds to the fields (31), differs a little from the relation (28) from Section 3. Hence it does not contradict the mechanism of the dispersion curves splitting that is now under discussion. The set of equations (31) describes the linearly polarized hybrid waves that asymptotically (when $\eta \to 0$) turn into the modes of the unchiral parallel-plate waveguide.

Let us note one property, which is characteristic of the behavior of $\xi_{[\pm n]}$ in the A-region. The strong analysis of the dispersion equations (16) and (17) shows the following. Let n, p be positive integral numbers and $n(1+\eta) < p < 2n$. Then there are values of the parameter $k_c a = \pi\sqrt{n(p-n)}/\sqrt{\eta}$, under which the equations (16) and (17) have equal roots $\tau_n = \left(p\sqrt{\eta}\right) / \left(2\sqrt{n(p-n)}\right)$. It means that under these values $k_c a$ the propagation constants from (18) coincide and this leads to intersections of the dispersion curves with different signs ($\pm$) (see Fig. 3b).

Now let us analyze the following moment in detail. It follows from Fig. 3b that all dispersion curves cross the straight line $k_c a = k_{-a}$, and the straight line $k_c a = k_{+a}$ is their common asymptote. It follows therefrom that when $k_c a \to \infty$ all chirowaveguide modes must be RHCP-waves and one might talk about a peculiar mode selection in a chirowaveguide. Therefore we will analyze in detail the dispersion and structure of the modes when $\rho \to \infty$. As follows from (1) and (20) the functions $U_{\pm}(y)$, which are solutions of the problem (7) and (8), can be represented in the form:

$$
\begin{aligned}
U_{-}(y) &= A_3 \left[\exp\left(-2\,(y/a)\,\rho \sin\varphi\right) + \exp\left(-2(1-y/a)\rho\sin\varphi\right)\right], \\
U_{+}(y) &= -A_3 \left[(1+\exp\left(-2\rho\sin\varphi\right)) \cos\left(2\frac{y}{a}\rho\cos\varphi\right)\right. \\
&\quad \left. + \tan\varphi \frac{1+\eta}{1-\eta}(1-\exp(-2\rho\sin\varphi)) \sin\left(2\frac{y}{a}\rho\cos\varphi\right)\right], \quad (32)
\end{aligned}
$$

where A_3 is the constant, and φ is the solution of the equation (20). Moreover from (20) we shall obtain that under $\rho \to \infty$ the following asymptotic formula is correct for all solutions:

$$\cos\varphi_n = [\pi(2n+1)/2\rho]\left[1-(1-\eta)(1+\eta)^{-1}\rho^{-1}+0\left(\rho^{-1}\right)\right], \quad (33)$$

where $n = 0, 1, 2, 3, \ldots$. The value φ_n with zero index corresponds to the mode with zero critical frequency. Substituting (33) into (22) it is easy to obtain the asymptotic formula for propagation constants:

$$\begin{aligned}\xi_{[+n]}a &= (1+\eta)\sqrt{(k_ca)^2-\pi^2(2n+1)^2}\left[1+\frac{\pi^2(2n+1)^2(1-\eta)}{(1+\eta)\sqrt{\eta}(k_ca)^2}\right.\\ &\left.+0\left(\left(\frac{\pi(2n+1)}{k_ca}\right)^2\right)\right], \quad (34)\end{aligned}$$

It is supposed in (34) that $k_ca \gg \pi(2n+1)$. The similar formula is for the solution of the equation (21) too, namely:

$$\xi_{[-n]}a = (1+\eta)\sqrt{(k_ca)^2-\pi^2(2n)^2}\left[1+\frac{\pi^2(2n)^2(1-\eta)}{(1+\eta)\sqrt{\eta}(k_ca)^2}+0\left(\left(\frac{2\pi n}{k_ca}\right)^2\right)\right], \quad (35)$$

where $k_ca \gg 2n\pi$ and $n = 1, 2, 3, \ldots$. It follows from (34) and (35) that under $\rho \to \infty$ all solutions of the dispersion equations (20) and (21) in the region B tend asymptotically to the propagation constant k_+ of the RHCP-wave in the infinite unchiral medium that does not contradict to (27).

Now we will consider the electromagnetic field structure of the chirowaveguide modes when $\rho \to \infty$. Here we shall restrict ourselves to the case of the dispersion equation (20) (the result will be the same in case of the equation (21)). Substituting (33) into (32) and taking into account the formulas (9) we shall obtain the asymptotic representation for components of the electric and magnetic fields with the accuracy of $0\left(\tilde{\rho}_n^{-1}\right)$ and of the multiplier $\exp(iz\xi_{[+2n+1]})$:

$$\begin{aligned}E_{+x} &= -A_3\left[2\tilde{\rho}_n\left(\frac{1+\eta}{1-\eta}\right)\sin\left(\pi(2n+1)\frac{y}{a}\right)+\left(1-2\frac{y}{a}\right)\right.\\ &\left.\cos\left(\pi(2n+1)\frac{y}{a}\right)-\exp(-2\rho y/a)-\exp\left(-2\rho(1-y/a)\right)\right],\\ E_{+y} &= -\frac{iA_3(1+\eta)}{1-\eta}\left[2\tilde{\rho}_n\sin\left(\pi(2n+1)\frac{y}{a}\right)+\left(\frac{1-\eta}{1+\eta}\right)\left(1-2\frac{y}{a}\right)\right.\\ &\left.\cos\left(\pi(2n+1)\frac{y}{a}\right)-\exp(-2\rho y/a)-\exp\left(-2\rho(1-y/a)\right)\right],\end{aligned}$$

$$
\begin{aligned}
E_{+z} &= [2A_3\sqrt{\eta}/(1-\eta)]\Big[\cos(\pi(2n+1)y/a) \\
&\quad -\exp(-2\rho y/a)+\exp\left(-2\rho(1-y/a)\right)\Big], \\
H_{+x} &= \frac{iA_3}{W}\left[2\tilde{\rho}_n\left(\frac{1+\eta}{1-\eta}\right)\sin\left(\pi(2n+1)\frac{y}{a}\right)+\left(1-2\frac{y}{a}\right)\right. \\
&\quad \left.\cos\left(\pi(2n+1)\frac{y}{a}\right)+\exp(-2\rho y/a)+\exp\left(-2\rho(1-y/a)\right)\right], \\
H_{+y} &= -\frac{A_3(1+\eta)}{W(1-\eta)}\left[2\tilde{\rho}_n\sin\left(\pi(2n+1)\frac{y}{a}\right)+\left(\frac{1-\eta}{1+\eta}\right)\left(1-2\frac{y}{a}\right)\right. \\
&\quad \left.\cos\left(\pi(2n+1)\frac{y}{a}\right)-\exp(-2\rho y/a)-\exp\left(-2\rho(1-y/a)\right)\right], \\
H_{+z} &= -\left[2iA_3\sqrt{\eta}/(W(1-\eta))\right]\Big[\cos(\pi(2n+1)y/a) \\
&\quad +\exp(-2\rho y/a)-\exp\left(-2\rho(1-y/a)\right)\Big]. \qquad (36)
\end{aligned}
$$

Here $\xi_{[+2n+1]} \approx h_{+2n+1} + K'_{+2n+1}$, $\tilde{\rho}_n = \rho/(\pi(2n+1))$. As follows from (36) the electric and magnetic fields are connected by the relation $\vec{H} = -(i/W)\vec{E}$ within the accuracy $0(\tilde{\rho}_n^{-1})$, and the electric field satisfies the equation $rot\ \vec{E} = k_+\vec{E}$ with the same accuracy. Hence the modes fields with the propagation constants $\xi_{[+n]}$ that satisfy the condition $k_- < \xi_{[+n]}, k_+$ are RHCP-waves under $\rho \to \infty$. The same result can be obtained for the $\xi_{[-n]}$ modes from the analysis of the equation (21).

So it follows from (25), (26), (31) and (36) that the field distribution of the chirowaveguide mode does not remain while the operating point moves along the dispersion curve. For example, the main $\xi_{[0]}$ mode under when $k_c a \to 0$ has the field distribution and the dispersion of the quasi-static TEM-wave (see (26)). While $k_c a$ increases it turns into the quasi-TEM hybrid mode (see (25)) and its dispersion begins to look like the dispersion of TE-waves of unchiral waveguides and, eventually, when $k_c a \to \infty$ it becomes the RHCP-wave with dispersion $\xi_{[0]} \to k_+$. The asymptotic character of the $\xi_{[0]}$ mode dispersion is not typical for quasi-static waves of the double-wire transmission lines [16, 17].

6. COUPLED MODES, MODE TRANSFIGURATIONS

From Sections 3–5 of this investigation it follows that the wavenumber $\xi_{[\pm n]}$ of the parallel-plate chirowaveguide satisfies the root dispersion (as h_n of the unchiral waveguide does) under all $0 < k_c a < k_+ a$. But

two kinds of dispersion: ζ-dispersion under small $\xi_{[\pm n]}$ (see (28)) and ξ-dispersion (see (27)) under large $\xi_{[\pm n]}$ are peculiar to a chirowaveguide. When $k_c a \to \infty$ the ξ-dispersion turns asymptotically into the k_+-dispersion of the infinite chiral medium. The dispersion curves of the parallel-plate chirowaveguide obtained using different ways for five lowest types of waves are shown in Fig. 4. Fig. 4a corresponds to the $\xi_{[0]}$-wave. It can be seen that $\xi_{[0]}$ begins as the dispersion of TEM-wave does. But the linearly polarized waves in the chiral medium cannot exist and $\xi_{[0]}$ turns fluently to the dispersion of the first waveguide mode ξ_{+1} while a increases. The similar transitions take place at the higher modes too (see Fig. 4). At that the dispersion type modification is accompanied by the modification of the field distribution and polarization (see Section 5). Let us refer these modifications to the mode transfiguration of the chirowaveguide. It is very typical for chiro-waveguides because the mode transfiguration may be observed at all chirowaveguide waves. Moreover it may be observed at many waves more than one time (see Fig. 4e). This leads to the complex character of the final dispersion curves behavior, to the dispersion type modification and to the mode polarization modification while moving an operating point along the dispersion curve, to intersections of the dispersion curves and to polarization selection etc. By that the chirowaveguide waves differ fundamentally from waves of unchiral waveguides and of other electrodynamic structures [16–20]. By the way, they differ also from plasma waveguides (the ungyrotropic case [21]) and from the waveguides with artificial unchiral dielectrics [22]. In all mentioned cases the form of the mode eigenfunction remains under any $k_c a$, though exclusions may take place. For example, in the waveguides, which are partially filled with dielectric [23, 24], transitions of the final dispersion curve from one branch to another occur (in [24] it was referred to as critical frequencies exchange). The transitions in [24] are also accompanied by the wave type change (for example, from H_{0m} to EH_{1m}).

Let us refer to the chirowaveguide modes as changeable waves. As it was mentioned above and in [7–10] all chirowaveguide modes are hybrid ones. Such waves are accepted to denote by the letters HE with corresponding indices. The traditional system of modes classification for a chirowaveguide seems to be illogical. It is illogical to number these waves in the usual manner, since because of intersections of the dispersion curves we have to stipulate every time in which sense (or when) the chosen number is smaller and when it is larger. It is proposed to put two indices near the letters HE: the upper one and the lower one, moreover the lower index must correspond to the initial number n (when $\xi_{[\pm n]} \to 0$) and the upper index must correspond to the

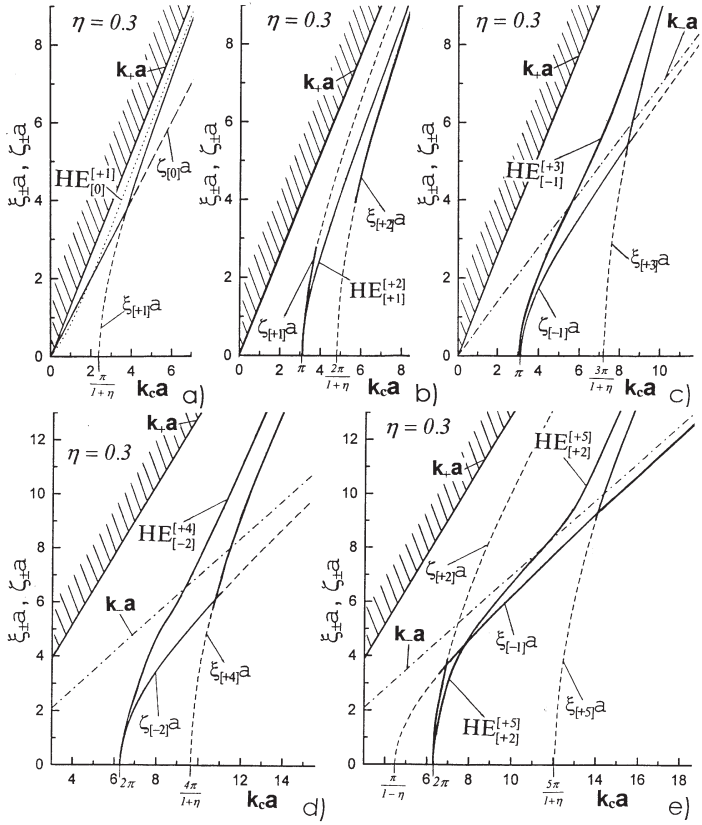

Figure 4. The mode transfiguration in the parallel-plate chirowaveguide for five lowest modes; the dispersion curves calculated using the formulas (27), (28), (10) and (11).

finite number m, which will be obtained after all transfigurations when $\xi_{[\pm n]} \to \infty$. The indices signs will denote the initial and final types of polarization, at that the sign (+) will correspond to the RHCP-wave and the sign (−) will correspond to the LHCP-wave. Let us note that the upper index sign can be omitted because it will always be the sign (+). Then the $HE^{[+1]}_{[0]}$ wave (see Fig. 4a) that goes out from the point $k_c a = 0$ will be the main wave of the parallel-plate chirowaveguide, and the next waves will be waves $HE^{[+2]}_{[+1]}$ (see Fig. 4b) and $HE^{[+3]}_{[-1]}$ (see Fig.4c) that go out from the point $k_c a = \pi$, and waves $HE^{[+4]}_{[-2]}$ (see Fig. 4d) and $HE^{[+5]}_{[-2]}$ (see Fig. 4e) that go out from the point $k_c a = 2\pi$

respectively. Then the waves $HE_{[+3]}^{[+7]}$ and $HE_{[-3]}^{[+6]}$ will come next (they are not shown in figures), they go out from the point $k_c a = 3\pi$ etc. The chirowaveguide modes will form pairs of the dispersion curves, which go out from points $k_c a = n\pi$: $HE_{[+n]}^{[2n+1]}$ and $HE_{[-n]}^{[2n]}$ (except for $n = 1$ when there is no intersection of the dispersion curves). As a result it is difficult to draw a distinction between the odd and even waves.

The phenomenon of dispersion curves splitting into pairs was referred to as the mode bifurcation in the works [7–10]. We could find the reason of this phenomenon. The wave splitting in a chirowaveguide takes place because the chiral medium with spatial dispersion provides coupling of different components of the wave field. It was succeeded in calculating the value of the coupling coefficient K_n that turned out to be proportional to the relative parameter of chirality. Then the mode bifurcation can be represented as the coupled modes splitting plus the mode transfiguration. Moreover this connection is provided by the medium with spatial dispersion. By the way the splitting of k_0 into $k_\pm$ in the infinite chiral medium is a phenomenon of the same type. The first cause of these splittings can be found in material equations for the chiral medium.

It follows from Figures 3 and 4 that all dispersion curves $\xi_{[\pm n]}$ cross the line $k_c a = k_- a$ (and tend asymptotically to the line $k_c a = k_+ a$) i.e., they hit into the region where only the RHCP-waves can exist. In other words the parallel-plate chirowaveguide performs polarization selection of the mode and when $\xi_{[\pm n]} > k_-$ it leaves only RHCP for all modes. Only separate parts of the dispersion curves correspond to the LHCP-wave. All these parts are situated below the line $k_c a = k_- a$ (see Fig. 4 also). However it does not mean the prohibition for LHCP under large $k_c a$. Under the arbitrary large $k_c a$ one can always find the mode with sufficiently large value of the lower index n, which will be able to transfer the LHCP-power; all other waves existed in a waveguide under the given $k_c a$ will be RHCP-waves. By that the chirowaveguide differs fundamentally from the infinite chiral medium, for which both polarizations are equivalent (see (2) and (3)). At the same time we shall note that in case of the circular chirowaveguide [5, 10] all dispersion curves cross the line $k_c a = k_- a$ too and hit into the region B.

7. CONCLUSION

It has been shown that the relative parameter of chirality η has a twofold physical meaning, it can determinate the coupling coefficient of polarizations or it can be included in the expression for ε_{eff}. And if for the infinite chiral space the selection of the physical meaning

of η is a matter of taste, in case of the chirowaveguide it leads to two different types of dispersion that determinate the final dispersion curves behavior at different lengths.

The modes transfiguration are typical for chirowaveguides. It has something in common with mode coupling [25, 26] but it has a whole series of strong distinctions and features. This phenomenon is a typical feature of chirowaveguides because it may be observed at all chirowaveguide waves without exception. Moreover it may be observed at many waves more than one time. This leads to the complex character of the final dispersion curves behavior, to modification of the wave type, dispersion type and the mode polarization while moving an operating point along the dispersion curve, and also to intersections of the dispersion curves and to polarization selection etc. The chiral medium in the region $\xi_{[\pm n]} \leq k_-$ entangles and interlaces the waves ξ_{+n} with ζ_{-n} and ξ_{-n} with ζ_{+n} due to the mode transfiguration. As a rule the waves with different dispersion ($\xi_{[\pm n]}$-waves with the waves $\zeta_{[\pm n]}$) and/or the waves with different index sign (i.e., with different polarization) take part in the mode transfiguration. On the one hand the ξ-dispersion and the ζ-dispersion are only certain representations of $\xi_{[\pm n]}$ that work in the different ranges of values: the ξ-dispersion works when $\xi_{[\pm n]} \to \infty$ and the ζ-dispersion works when $\xi_{[\pm n]} \to \infty$. On the other hand the ξ- and ζ-branches behave as they are independent waves. So the ζ_{-1}-branch takes part in the forming of the $HE_{[+1]}^{[+2]}$ mode and the ξ_{-1}-branch takes part in the forming of the $HE_{[+2]}^{[+5]}$ mode. There is another example: ζ_{+1} takes part in the forming of the $HE_{[+1]}^{[+2]}$ mode and ξ_{+1} takes part in the forming of the $HE_{[0]}^{[+2]}$ mode. Moreover, the first three modes $HE_{[0]}^{[+1]}$, $HE_{[+1]}^{[+2]}$ and $HE_{[-1]}^{[+3]}$ represent rather extrinsic situation of the mode transfiguration. The typical situation is possible to see starting with the $HE_{[+2]}^{[+5]}$ and $HE_{[-2]}^{[+4]}$ wave types (more than five wave types take part in the mode transfiguration forming an intersection of two final dispersion curves) (see Fig. 4 also). Moreover the number of intersections increase while n grows. In the unchiral waveguide the wave dispersion is determined by the angle θ dependence on $k_c a$. In the chirowaveguide the dispersion is determined both by the angle θ dependence on $k_c a$ and by the mode transfigurations.

The mode transfiguration leads to the polarization selection of circular polarization waves. By that the chirowaveguide differs from the infinite chiral medium. If in the chiral medium both the LHCP and RHCP polarizations are equivalent then in the chirowaveguide the preference is given to the right spiral (RHCP). It is interesting that in

the bioorganic world the macromolecules homochirality does not have exclusions [27–29]; macromolecules of ferments, RNA, DNA etc. are constructed from parts with the same chirality sign. It is usually told about the chiral specificity of the bioorganic world. But the generally accepted explanation of the property of bioorganic molecules has not been formulated yet.

ACKNOWLEDGMENT

We express our thanks to doctor Nader Engheta, University of Pennsylvania, Philadelphia, USA, to professor S. A. Masalov, Usikov Institute for Radiophysics & Electronics National Academy of Sciences, Kharkov, Ukraine and to professor N. P. Yashina, Universite Blaise Pascal de Clermont-Ferrand, France, for their interest in this work and for useful discussion.

REFERENCES

1. Jaggard, D. L. and N. Engheta, "Chirality in electrodynamics: modelling and applications," *Directions in Electromagnetic Wave Modelling*, H. L. Bertoni and L. B. Felsen (Eds.), Plenum Publishing Co., New York, 1993.
2. Lakhtakia, A., "The Maxwell postulates and chiral worlds," collection of papers: *Essays on the Formal Aspects of Electromagnetic Theory*, A. Lakhtakia (Ed.), 747–755, World Scientific Publishing Co. Pte. Ltd., 1993.
3. Mariotte, F., S. A. Tretyakov, and B. Sauviac, "Modeling effective properties of chiral composites," *IEEE Trans. Antennas and Propagation Magazine,* Vol. 38, No. 2, 22–32, April 1996.
4. He, S., M. Norgren, and T. Takenaka, "Trace formalism and explicit gradients for parameter reconstruction/design of a stratified bianisotropic slab/coating," *Journal of Electromagnetic Waves and Applications,* Vol. 13, 631–647, 1999.
5. Lindell, I. V., A. Sihvola, S. A. Tretyakov, and A. J. Viitanen, *Electromagnetic Waves in Chiral and Bi-isotropic Media,* 332, Artech House Inc., Boston, London, 1994.
6. Lakhtakia, A., V. K. Varadan, and V. V. Varadan, "Time-harmonic electromagnetic fields in chiral media," *Lecture Notes in Physics*, Vol. 335, 121, Springer-Verlag, Berlin, 1989.
7. Engheta, N. and P. Pelet, "Modes in chirowaveguides," *Opt. Lett.,* Vol. 14, No. 11, 593–595, 1989.

8. Pelet, P. and N. Engheta, "The theory of chirowaveguides," *IEEE Trans. Antennas Propagat.,* Vol. AP-38, No. 1, 90–98, 1990.
9. Mahmoud, S. F., "On mode bifurcation in chirowaveguide with perfect electric walls," *J. Electromagnetic Waves Appl. (JEWA),* Vol. 6, No. 10, 1381–1392, 1992.
10. Svedin, J. A. M., "Propagation analysis of chirowaveguides using the finite-element method," *IEEE Trans. Microwave Theory Tech.,* Vol. MTT-38, No. 10, 1488–1496, Oct. 1990.
11. Kluskens, M. S. and E. H. Newman, "A microstrip line on a chiral substrate," *IEEE Trans. Microwave Theory Tech.,* Vol. MTT-39, No. 10, 1889–1891, Nov. 1991.
12. Li, L. W., M. S. Leong, P. S. Kooi, T. S. Yeo, and K. H. Tan, "Rectangular modes and dyadic green's functions in a rectangular chirowaveguide," *IEEE Trans. Microwave Theory Tech.,* Vol. MTT-47, No. 11, 67–81, January 1999.
13. Ditchburn, R. W., *Light,* 631, Blackie & Son Limited, Glasgow, London, 1952.
14. Marcatili, E. A. I., "Dielectric rectangular waveguide and directional coupler for infrared optics," *Bell System Tech. J.,* Vol. 48, 2071–2079, 1969.
15. Komar', G. I., "Slot wave of the coupled cylindrical and image slot lines and the directional couplers based on them," *Izvestiya VUZov, Radiophizika,* Vol. 32, No. 4, 492–501, Russian, Apr. 1989.
16. Southworth, G. C., *Principles and Applications of Waveguide Transmission,* 670, New York, 1950.
17. Ramo, S. and J. R. Whinnery, *Fields and Waves in Modern Radio,* 631, New York, 1944.
18. Komar', G. I., "On eigen values and functions of the leaky wave," presented at the *XXIIIrd URSI General Assembly,* Vol. 2, 398, Prague, Czechoslovakia, Aug. 28–Sept. 5, 1990.
19. Masalov, S. A, A. V. Ryzhak, O. I. Sukharevskiy, and V. M. Shkil', *The Physical Fundamentals of the Wide-Band Technologies of the Stells Type,* 163, Publishing House of A. F. Mozhaiskiy MES University, Sankt-Peterburg, Russian, 1999.
20. Shestopalov, V. P., Yu. A. Tuchkin, A. Yu. Poyedinchuk, and Yu. K. Sirenko, *The New Nethods of Solving the Direct and Inverse Problems of the Diffraction Theory. The analytic regularization of the electrodynamic boundary problem,* 284, Kharkov University Publishers, Kharkov, Russian, 1997.
21. Kondratenko, A. I., *The Plasma Waveguides,* 232, Atomizdat, Moscow, Russian, 1976.

22. Fainberg, Ya. B. and N. A. Hizhnyak, "The artificial anisotropic media," *Zhurnal Tehnicheskoy Fiziki,* Vol. 25, No. 4, 711, Russian, 1955.
23. Clarricoats, P. J. B., "Backward waves in waveguides containing dielectrics," *Proc. IEE,* Vol. 108C, No. 14, 496–501, 1961.
24. Ilarionov, Yu. A., S. B. Raevskiy, and V. Ya. Smorgonskiy, "The computation of the corrugated and partially filled waveguides," *Sovetskoe Radio,* V. Ya. Smorgonskiy (Ed.), 200, Moscow, Russian, 1980.
25. Melezhik, P. N., A. Yu. Poyedinchuk, et al., "The analytical nature of the effect of the natural oscillations mode coupling," *USSR Acad. of Sciences Reports,* Vol. 300, No. 6, 1356–1359, Russian, 1988.
26. Pochanina, I. E., V. P. Shestopalov, and N. P. Yashina, "The interaction and degeneration of the natural oscillations of the open waveguide resonators," *USSR Acad. of Sciences Reports,* Vol. 320, No 1, 90–95, Russian, 1991.
27. Avetisov, V. A. and V. I. Goldanskiĭ, "Physical aspects of mirror symmetry breaking in the bioorganic world," *Uspekhi Fizicheskikh. Nauk (UFN),* Vol. 166, No. 8, 873–891, Russian, August 1996.
28. Chernavskiĭ, D. S., "The origin of life and thinking from the modern physics point of view," *Uspekhi Fizicheskikh. Nauk (UFN),* Vol. 170, No. 2, 157–183, Russian, February 2000.
29. Holmstedt, B., H. Frank, B. Testa, and A. R. Liss, *Chirality and Biological Activity,* New York, 1990.